



## Capillary absorption in concrete and the *Lucas–Washburn* equation

Lucija Hanžič<sup>a,\*</sup>, Ladislav Kosec<sup>b</sup>, Ivan Anžel<sup>c</sup>

<sup>a</sup> Faculty of Civil Engineering, University of Maribor, Smetanova 17, 2000 Maribor, Slovenia

<sup>b</sup> Faculty of Natural Sciences and Engineering, University of Ljubljana, Aškerčeva 12, 1000 Ljubljana, Slovenia

<sup>c</sup> Faculty of Mechanical Engineering, University of Maribor, Smetanova 17, 2000 Maribor, Slovenia

### ARTICLE INFO

#### Article history:

Received 30 January 2009

Received in revised form 7 October 2009

Accepted 12 October 2009

Available online 17 October 2009

#### Keywords:

Capillary absorption

*Lucas–Washburn* equation

Concrete

Neutron Radiography

### ABSTRACT

Capillary absorption kinetics of concrete–ethylene glycol system was studied with respect to concrete matrix porosity and liquid viscosity. Porosity of specimens was altered by air-entraining agents and superplasticizers. Liquid which doesn't react with cement gel was chosen for the experiment in order to study the reasons for deviation from *Lucas–Washburn* equation observed in concrete–water system. Viscosity of ethylene glycol changes from ~23 to 2 mPa s in the temperature range from 20 to 100 °C. The values of the capillary coefficient were determined at 20, 60 and 100 °C using Neutron Radiography and were found to be in the range from ~1.5 to 4.9 mm h<sup>-1/2</sup>. The results show that the *Lucas–Washburn* equation in concrete–ethylene glycol system is valid only for ~25 h, which indicates that swelling and rehydration of cement gel are not the main reasons for deviation observed in concrete–water system.

© 2009 Elsevier Ltd. All rights reserved.

### 1. Introduction

Moisture is one of the major factors that contribute to deterioration of concrete. Transport of liquids in porous media such as concrete takes place in open pores mainly due to diffusion, suction and capillary absorption. The driving forces of the diffusion and suction processes are concentration and the pressure gradient, respectively, whereas capillary absorption is driven by surface tension.

Diffusion is the prime mechanism when the liquid concentration in a porous medium is low and movement of discrete liquid particles (molecules) is analysed. However, when suction or capillary absorption are studied, the liquid is considered to be a continuum characterized by its viscosity. Suction is the prime mechanism in systems of high liquid concentration and takes place in larger pores, where surface tension is negligible in comparison to forces resulting from the pressure gradient. On the other hand, capillary absorption takes place in fine pores (10 nm–10 μm), where forces arising from surface tension are in the same range as gravity forces present in the liquid. It is the prime mechanism when the material is only partially wetted, and is usually described by the *Lucas–Washburn* equation [1,2]:

$$h = k\sqrt{t} \quad (1)$$

where  $h$  is height of the liquid front (m),  $t$  is the wetting time (s) and  $k$  is the capillary coefficient (m s<sup>-1/2</sup>). In the *Lucas–Washburn* equation, the capillary coefficient is defined as:

$$k = \sqrt{\frac{\gamma r \cos \theta}{2\eta}} \quad (2)$$

where  $\gamma$  is the surface tension (N m<sup>-1</sup>),  $r$  the capillary radius (m),  $\theta$  the contact angle (°) and  $\eta$  the dynamic viscosity (Pa s).

In principle, all the parameters constituting the capillary coefficient can be measured independently, and thus values of  $k$  can be calculated. However, determination of the capillary radius in porous materials is quite controversial. Actual porosity of concrete as observed by microscope only remotely resembles the three dimensional network of circular tubes which is used to model porosity. For this reason Jankins and Rao introduced a geometric factor to take into account shape variations [3], but it was later shown by Cook and Hover that its effect is negligible for cementitious materials [4]. In addition, Maage proved that circular representation of pores is most adequate [5]. Even though a circular cross section of capillary tubes can be adopted, the fact remains that distribution of their radii covers a broad range.

In order to estimate a single-value characteristic pore radius, Atzeni et al. suggested calculation of the mean distribution radius [6], Reinhardt and Gaber proposed the equivalent pore radius [7], whereas Schoelkopf et al. introduced the representative pore radius [8]. Still, these values differ and they also depend on the technique used for porosity measurements. In addition, the study carried out by Schoelkopf et al. [8] using calcium carbonate and mineral oil indicated that not all the pores are filled simultaneously and that the selective pathway for liquid transport is the result of liquid inertia and the acceleration gained by the liquid at the entrance of each pore.

\* Corresponding author. Tel.: +386 2 22 94 331; fax: +386 2 25 24 179.

E-mail address: [lucija.hanzic@uni-mb.si](mailto:lucija.hanzic@uni-mb.si) (L. Hanžič).

Complex issues also arise when contact angle between liquid and solid phase is considered. Although macroscopic contact angle can be determined using a rather simple static sessile drop method, long range van der Waals forces in capillary tubes can cause a difference between microscopic and macroscopic contact angle. Additionally, nano-scaled roughness of capillary walls and the velocity of liquid movement have a significant effect on the contact angle value [9]. Moreover, derivation of *Lucas–Washburn* equation from a physical model is based on the presumption that gravity can be neglected, whereas the friction between liquid and solid is not considered. Based on these facts it can be concluded that values of  $k$  are more reliable if they are measured directly.

Because of difficulties associated with capillary coefficient measurements, the gravimetric method is usually applied and sorptivity  $S$  ( $\text{m s}^{-1/2}$ ) is determined according to:

$$i = S\sqrt{t} \quad (3)$$

where  $i$  is the volume of absorbed liquid per unit cross section ( $\text{m}$ ). However, it should be noted that values of  $S$  and  $k$  may differ significantly [10]. For instance, when an air-entraining agent is added to concrete, its apparent porosity is increased and such concrete absorbs a large amount of liquid which results in high values of sorptivity. But bubbles in air-entrained concrete cause disconnection of the capillary network and act as small storage tanks. Liquid is therefore detained in the lower region and the values of capillary coefficient are low. In order to avoid these problems, the Neutron Radiography (NR) is used in this study and values of  $k$  are determined.

Independent studies of capillary absorption of water in concrete have shown a significant deviation from the *Lucas–Washburn* equation [10–13]. It was established, that after a certain time, capillary absorption decelerates. Taylor et al. [13] assigned this effect to the swelling associated with the hydration and rehydration of unreacted and dehydrated components constituting the hardened cement paste. This argument is reasonable, since experiments performed on concrete using organic liquids did not show a similar deviation [10,12,13]. Yet, the exposure time in the majority of these experiments was rather short and deviation, although it might exist, was not detected.

Therefore, the aim of this study was to determine whether the above stated mechanisms are of major importance for deviation from *Lucas–Washburn* equation in concrete–water system. If so, deviation should not occur in concrete–organic liquid system even after longer wetting periods. Since concrete is often used for construction of barriers that are supposed to prevent contamination of soil by organic liquids (e.g. oil storage tanks), the question whether such a liquid is going to propagate through concrete in agreement with the *Lucas–Washburn* equation even after a long time of exposure is not a matter of scientific curiosity only.

The paper presents a study of capillary absorption of ethylene glycol carried out on three different types of concrete matrix. The influence of its porosity and liquid viscosity on capillary coefficient is studied.

## 2. Experimental

### 2.1. Method

In the framework of this capillary absorption study using NR, the height of the liquid front, as well as the concentration of the liquid inside the specimen are determined. The applicability of NR for measurements of capillary absorption in concrete is based on the fact that concrete components are composed of elements which only attenuate a thermal neutron flux to a small degree. Hence, when irradiated with neutrons having energies of approxi-

mately 25 meV (thermal neutrons), concrete is rather transparent. On the other hand, hydrogen, which is the main constituent of water and organic liquids, attenuates a thermal neutron flux to a much higher degree. Therefore, a marked contrast between dry and wet part of the specimen is observed on neutron radiographs.

The interaction of thermal neutrons with hydrogen atoms is mainly by elastic scattering where the mean scattering angle is established to be  $\sim 50^\circ$  [14]. Therefore, the neutron detector must be placed behind the specimen at a distance large enough to avoid detecting scattered neutrons but close enough to capture a sharp image.

NR experiments were performed using the thermal column at the *TRIGA Mark II* reactor of the *Jožef Stefan Institute* in Ljubljana. At the irradiation site, the functional diameter of the neutron beam is 90 mm and the thermal neutron flux is  $\sim 4 \times 10^5 \text{ cm}^{-2} \text{ s}^{-1}$  (measured with an Au foil). Detection of neutrons was performed with a *FUJI IP\_ND* imaging plate, which was placed 8 cm behind the specimen. A *FUJI BAS 1500* laser scanner was used to transfer the image from imaging plate into computer and a digital image containing Photo-Stimulated Luminescence (PSL) values was obtained. The height of the liquid front was measured on the digital images using the *TINA 2.10g* computer program (*Isotopenmeßgeräte GmbH*, 1993).

In order to determine the liquid concentration in porous material, the following consideration is made. When a neutron beam of initial flux  $\Phi_0$  ( $\text{n m}^{-2} \text{ s}^{-1}$ , where  $n$  stands for neutrons) strikes the observed object, some neutrons will interact with nuclei of the object and only part of the neutrons will pass through. The flux of uncollided neutrons ( $\Phi$ ) is calculated as:

$$\Phi = \Phi_0 e^{-\Sigma w} \quad (4)$$

where  $\Sigma$  is the macroscopic cross section ( $\text{m}^{-1}$ ) and  $w$  is the specimen thickness ( $\text{m}$ ) [14,15]. The neutron flux behind a specimen of a porous material with pores partially filled with liquid is calculated as:

$$\Phi = \Phi_0 e^{-(\Sigma_m + \hat{c}_l \Sigma_l)w} \quad (5)$$

where  $\Sigma_m$  is the macroscopic cross section of the material,  $\Sigma_l$  is the macroscopic cross section of the liquid and  $\hat{c}_l$  is the volumetric liquid content ( $\text{m}^3 \text{ m}^{-3}$ ) [16].

The signal  $\Omega$  ( $\text{PSL m}^{-2}$ ) recorded by the imaging plate depends on the neutron fluence  $\varphi$  ( $\text{n m}^{-2}$ ), which is the total number of neutrons that impinge on the detector per unit area and is calculated as:

$$\varphi = \int \Phi(t) dt \quad (6)$$

It was established by Kobayashi and Satoh [17] that the recorded signal is approximately proportional to the neutron fluence as:

$$\Omega = f \varphi^{0.974} \approx f \varphi \quad (7)$$

where  $f$  is the proportionality coefficient ( $\text{PSL n}^{-1}$ ). Hence, the macroscopic cross section of a material can be determined from Eq. (4) as follows:

$$\Sigma = \frac{-1}{w} \ln \frac{\Omega}{\Omega_0} \quad (8)$$

where  $\Omega_0$  is the signal caused by the initial beam and  $\Omega$  is the signal caused by the attenuated beam. The volumetric concentration of the liquid can be calculated from Eq. (5) as:

$$\hat{c}_l = \frac{-1}{\Sigma_l} \left( \Sigma_m + \frac{1}{w} \ln \frac{\Omega}{\Omega_0} \right) \quad (9)$$

The volumetric concentration is in principle defined as:

$$\hat{c}_l = \frac{V_l}{V} = p_a q \quad (10)$$

where  $V_l$  is the volume of the liquid inside the specimen ( $\text{m}^3$ ),  $V$  the specimen volume ( $\text{m}^3$ ),  $p_a$  the apparent porosity ( $\text{m}^3 \text{m}^{-3}$ ) and  $q$  the proportion of pores filled with liquid ( $\text{m}^3 \text{m}^{-3}$ ). Finally, the mass concentration of liquid in the porous material  $c_l$  ( $\text{kg m}^{-3}$ ) is defined as the liquid mass per unit volume of the specimen and is therefore calculated as:

$$c_l = \rho_l \hat{c}_l \quad (11)$$

where  $\rho_l$  is the liquid density ( $\text{kg m}^{-3}$ ).

## 2.2. Materials

Selection of the liquid for the experimental work was based on the following criteria:

1. the atomic proportion of hydrogen must be high in order to achieve good contrast between a dry and wet part of the specimen using NR;
2. the molar mass should be low so that the liquid may be considered as Newtonian;
3. in order to study the influence of liquid viscosity on capillary absorption kinetics, the viscosity should change significantly in the temperature range from 20 to 100 °C; and
4. for safety reasons the liquid should not be explosive and its boiling point and ignition temperature have to be high.

Ethylene glycol was found to be an optimal choice. According to its molecular formula ( $\text{C}_2\text{H}_6\text{O}_2$ ) the proportion of hydrogen atoms is 60 at.%, its molar mass is  $62 \text{ g mol}^{-1}$  whereas its boiling point and ignition temperature are 198 and 410 °C, respectively. Based on these data it was decided that experiments shall be performed at 20, 60 and 100 °C.

The kinematic viscosity of ethylene glycol was measured by a Cannon–Fenske viscometer. Since the density of ethylene glycol is 1.11, 1.08 and  $1.06 \text{ g cm}^{-3}$  at ~20, 60 and 100 °C, respectively, the dynamic viscosity at these temperatures is calculated to be 23.0, 5.2 and  $2.1 \text{ mPa s}$ . Thus, in studied temperature range density is reduced for 4.5%, whereas dynamic viscosity is reduced for 95%. Consequently, the change of gravity force is not of paramount importance when changes of capillary coefficient are considered.

Surface tension values of ethylene glycol in the air as determined by Jho and Carreras [18] are 47.3 and  $46.3 \text{ mN m}^{-1}$  at 25 and 40 °C, respectively. Since surface tension of organic liquids decreases with increasing temperature in almost linear manner [19], the calculated values for ethylene glycol are ~48, 45 and  $42 \text{ mN m}^{-1}$  at 20, 60 and 100 °C, respectively. Macroscopic contact angle between ethylene glycol and cementitious material at 20 °C was estimated to be ~35° using the static sessile drop method. However, when the cementitious substrate is saturated with ethylene glycol, its value approaches 0°.

Five types of cementitious specimens were prepared for experimental work namely, a reference mix, two mixtures with the air-entraining agents and two mixtures with the superplasticizers. All mixtures were obtained by mixing 1350 g of aggregate, 202.5 g of water and 450 g of Portland cement CEM I 42.5 R (designation defined by standard EN 197-1 [20]). Hence, the resulting water-to-cement ratio is 0.45.

The aggregate used was standard quartz sand which complies with EN 196-1 [21], thus having the maximum grain size of 2 mm. Coarse aggregate fractions were excluded upon the consideration regarding dimensional restrictions for specimens used for porosity and capillarity measurements. Due to the absence of coarse aggregate, the specimens can be considered as the concrete matrix which forms the continuous phase of the composite. Although there is some controversy over the influence of the interfacial transition zone on the permeability

of concrete, in general it is the bulk of the matrix that controls it [22] and conclusions of the study can be extended to the concrete itself.

The types and quantities of admixtures, as well as mixture designations, are given in Table 1. Three prisms with dimensions  $40 \text{ mm} \times 40 \text{ mm} \times 160 \text{ mm}$  were cast from each mixture. They were kept at  $20 \pm 2 \text{ °C}$  and 100% humidity for 28 days. After the curing period, the surfaces which were in contact with the mould were cut off and the prisms were cut longitudinally in halves. Hence, six basic specimens with dimensions somewhat smaller than  $20 \text{ mm} \times 40 \text{ mm} \times 160 \text{ mm}$  were obtained from each mixture. They were dried at 105 °C and stored in a desiccator at room conditions.

Specimens for porosity measurements were prepared from the basic specimens with a hammer and chisel. The force was therefore applied rapidly and on a small area. In such case cracks propagate more or less in one direction and do not spread throughout the specimen. Therefore, the amount of additional cracks can be considered negligible in comparison to existing porosity. One or two fragments with a total mass of ~2 g were selected for testing. The porosity of the specimens was determined by Mercury Intrusion Porosimetry (MIP) using a *Micro-metrics Pore Sizer 9310*, which can apply a maximum pressure of 207 MPa.

Basic specimens chosen for capillarity measurements were equipped with silicon markers as depicted in Fig. 1. The sides of the specimens, which were dipped into the liquid, were covered with a thin silicone coating ~1 cm high to prevent liquid absorption. Thus, liquid propagated into the specimen only through the bottom surface. The rest of the specimen was wrapped in aluminium foil, which is transparent for thermal neutrons, in order to prevent evaporation of the liquid, as well as invasion of moisture from the air into the specimen. Specimens were placed on a stand in the liquid container (see Fig. 1). The temperature of the whole system was regulated in an oven to  $\pm 3 \text{ °C}$  precision. The experiments were carried out at 20, 60 and 100 °C.

Vertical set-up was adopted despite the fact that *Lucas–Washburn* equation neglects the gravity by assuming a horizontal layout of a capillary tube. However, in porous media capillary tubes are oriented in all directions and even in the case of horizontal set-up where liquid front propagates from one side of the specimen, the flow inside each capillary tube is not strictly horizontal. Moreover, gravity forces cause the absorbed liquid to drain through the capillary network from the upper part of the specimen towards the bottom. In addition hydrostatic pressure increases with depth. So, the advance of liquid front in horizontal set-up is not uniform which was confirmed by preliminary experiments.

**Table 1**

Types and quantities of admixtures used for the preparation of concrete mixtures together with mixture designations.

Admixture type	Admixture name	Mixture designation	Relative quantity of admixture <sup>a</sup> (%)
No admixture	–	R	0
Air-entraining agent	Cementol	A <sub>S</sub>	0.3
	ETA S	A <sub>S1</sub>	0.3
	Cementol	A <sub>S1</sub>	0.3
Superplasticizer	ETA S1	S <sub>P</sub>	2.0
	Cementol	S <sub>P</sub>	2.0
	ZETA P	S <sub>T</sub>	2.0
	Cementol	S <sub>T</sub>	2.0
	ZETA T		

<sup>a</sup> According to the mass of cement.

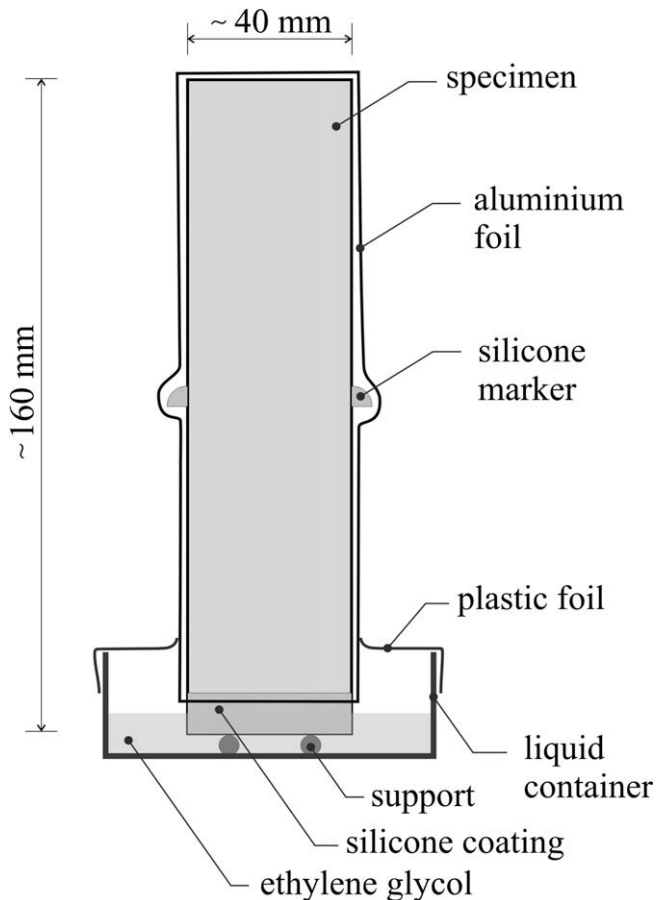


Fig. 1. Schematic representation of the specimen during capillary absorption measurements. The thickness of the specimen was ~20 mm.

### 3. Results and discussion

#### 3.1. Concrete porosity

The results of porosity measurements by MIP are summarized in Table 2. It may be seen that the apparent porosity increases by ~7% as the consequence of the air-entraining agent, but is not altered by addition of a superplasticizer. Nevertheless, the superplasticizers affect the distribution of pores according to their radius; namely pores are concentrated in the micro capillary class. On the other hand, the air-entraining agents cause a shift towards larger pores so that ~70% of them were larger than 0.1  $\mu\text{m}$ . This value amounts only to ~15% for the reference specimens and for those made with superplasticizer.

The shift in pore distribution of air-entrained specimens is reflected in the mean distribution radius ( $r_m$ ) calculated according to Atzeni et al. [6]:

$$\ln r_m = \frac{\sum V_i \ln r_i}{\sum V_i} \quad (12)$$

where  $V_i$  is the pore volume ( $\text{m}^3$ ) corresponding to radius  $r_i$  (m). As follows from Table 2, the values of mean distribution radius do not reflect the differences of pore distributions in specimens made with superplasticizer in comparison to the reference one.

#### 3.2. Capillary coefficient

For the determination of capillarity coefficient by NR, the height of the liquid front was measured in three vertical profiles either by measuring the distance directly on the digital neutronograph (Fig. 2a) or by using PSL values plotted against distance, as demonstrated in Fig. 2b. A schematic presentation of the results (see Figs. 3–5) show three more or less distinctive regions of capillary absorption.

In the initial stage a short dormant period can be observed. This period lasts ~1 h at 20 °C – temperature at which the viscosity of ethylene glycol is large; and is shortened when the viscosity decreases as a result of a temperature increase.

The dormant period is followed by a linear dependence between the height of the liquid front and the square root of time as stated by the Lucas–Washburn equation (Eq. (1)). The average duration of the second period in the reference specimen, as well as in specimens with superplasticizer at temperatures of 20, 60 and 100 °C is ~70, 90 and 30 h, respectively, whereas these values amount to 50, 50 and 10 h for specimens with air-entraining agent.

Values of the capillary coefficient are summarized in Table 3. The results show, that values of the capillary coefficient at 60 °C were approximately twice the values at 20 °C. When the temperature of the system is increased, the density and viscosity of ethylene glycol decrease. Hence, the forces of gravity and viscosity, which hinder liquid movement, decrease and the liquid is expected to rise higher at elevated temperature. However, due to the magnitude of change, namely density decreases for less than 2% in the 20–60 °C temperature range whereas viscosity decreases for more than 77%, the contribution of the latter is essential. Based on the assumption that the value of contact angle does not change significantly in this temperature range, the result stated above is found to be in accordance with Eq. (2).

When the temperature is raised to 100 °C, the viscosity of ethylene glycol is reduced by a factor of 11 whereas its surface tension is reduced by factor of 1.1. Thus, values of the capillary coefficient according to Eq. (2) should have been  $3.1 \times$  the values at 20 °C. However, this factor was found to be only 2.4 on average. This indicates that due to increased velocity of liquid movement the change in contact angle is significant and it was established that  $\cos \theta$  is reduced by a factor of 1.7 when the system is heated from 20 to 100 °C.

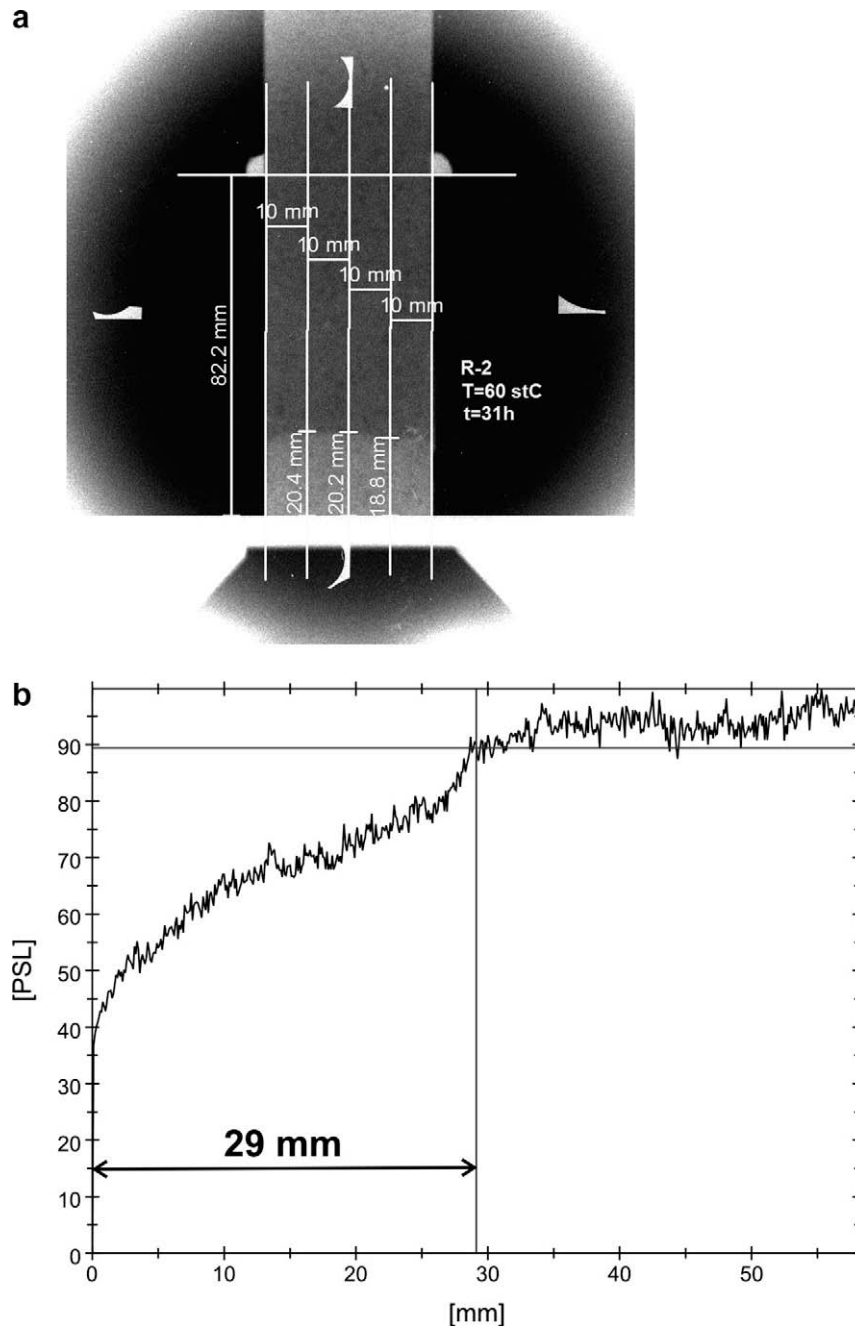
An analysis of capillary absorption with respect to the porosity of specimens showed that addition of air-entraining agents and superplasticizers alters the values of the capillary coefficient by

Table 2

Apparent porosity ( $p_a$ ), distribution of pores according to their diameter and mean distribution radius ( $r_m$ ) for reference concrete (R), concretes with air-entraining agents ( $A_S$ ,  $A_{S1}$ ) and concretes with superplasticizers ( $S_P$ ,  $S_T$ ) as determined by Mercury Intrusion Porosimetry.

Mixture	$p_a$ (%)	Gel pores (%) <10 nm	Capillary pores (%)			Voids (%) >10 $\mu\text{m}$	$r_m$ (nm)
			Micro 10–100 nm	Meso 100 nm–1 $\mu\text{m}$	Macro 1–10 $\mu\text{m}$		
R	14	8	76	12	3	1	28
$A_S$	20	2	28	61	6	3	95
$A_{S1}$	23	2	31	61	3	3	75
$S_P$	15	4	82	10	3	1	31
$S_T$	17	5	84	8	2	1	29





**Fig. 2.** Determination of the height of the liquid front using the *TINA 2.10g* computer program (*Isotopenmeßgeräte GmbH*, 1993): (a) visual determination of the liquid front and measurement of its distance from the bottom of the specimen; (b) determination of the liquid front using PSL (Photo-Stimulated Luminescence) profiles.

factors of 0.9 and 1.1 on average, respectively. This is in agreement with the prediction that larger pores, which represent the major portion of the apparent porosity of specimens with an air-entraining agent, are less important for capillary absorption. On the contrary, the higher concentration of pores in the micro capillary class, which is the result of superplasticizer addition, favours the process of capillary absorption.

Finally, in the third region of capillary absorption the transport of liquid is significantly slower than predicted by the *Lucas–Washburn* equation and the liquid front more or less levels off at a certain height. As predicted, the estimated maximum height is lower in specimens with an air-entraining agent than in other specimens. It is very probable that in this region diffusion mechanisms prevail over capillary absorption.

### 3.3. Liquid concentration

In order to determine the concentration of liquid in cementitious specimens according to Eq. (9), their macroscopic cross sections as well as macroscopic cross section of ethylene glycol were measured. Details are given in Ref. [23]. The specimens used in this study were found to have macroscopic cross sections in the interval from 0.31 to 0.37  $\text{cm}^{-1}$ , which is consistent with the value (0.33  $\text{cm}^{-1}$ ) reported by Pel [16]. The macroscopic cross section of ethylene glycol was found to be 1.50  $\text{cm}^{-1}$ .

In the NR system used for this study the contribution of scattered neutrons is negligible up to a thickness of 1 cm of ethylene glycol. Taking into account the mass of ethylene glycol absorbed by the specimens and the height to which it has risen, its equivalent

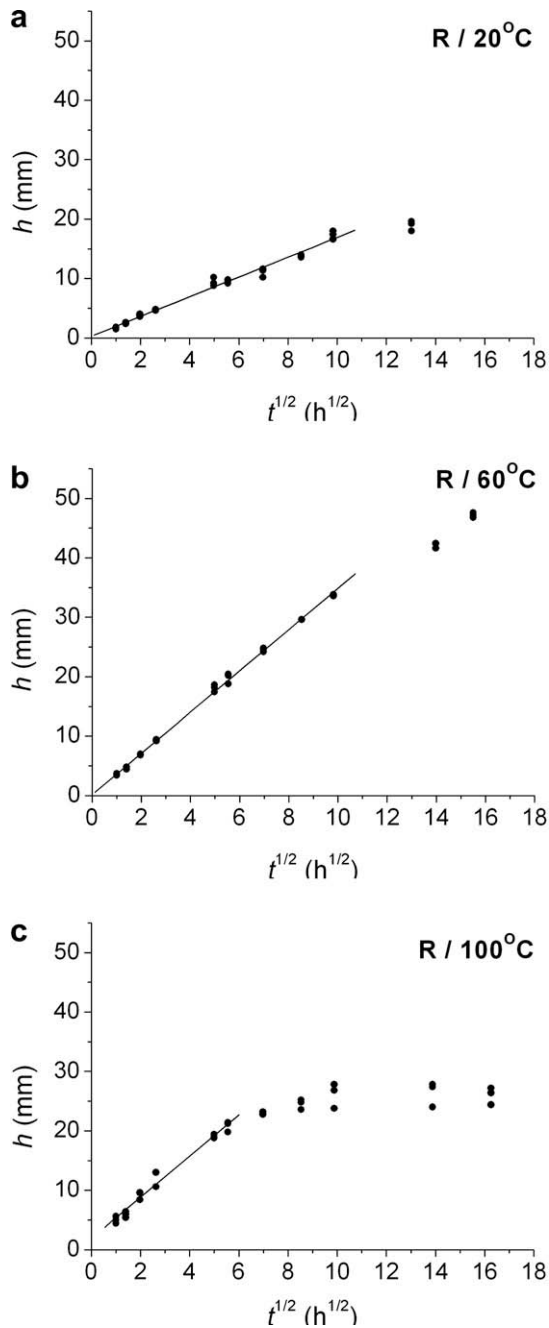


**Fig. 3.** Height of the liquid front ( $h$ ) versus the square root of time ( $t$ ) for the reference specimen (R) at: (a) 20 °C; (b) 60 °C and; (c) 100 °C.

thickness was estimated to be  $\sim 2$  mm. Thus, the contribution of scattered neutrons in the experiment is negligible and forms part of the background.

The concentration of liquid is determined in horizontal profiles every 5 mm from the bottom of the specimen. A characteristic set of results obtained 15 mm above the bottom edge of specimens R,  $A_S$  and  $S_T$  at 60 °C is depicted in Fig. 6. It may be observed that the liquid concentration in specimen  $A_S$  is significantly lower than the liquid concentration in specimens R and  $S_T$ , despite the fact that its apparent porosity is  $\sim 5\%$  higher.

As follows from Table 4 where the portions of pores actually filled with liquid ( $q_{act}$ ) are summarized, only 45% of the pores in specimen  $A_S$  are filled with ethylene glycol, whereas this value amounts to 88% and 72% for specimens R and  $S_T$ , respectively.

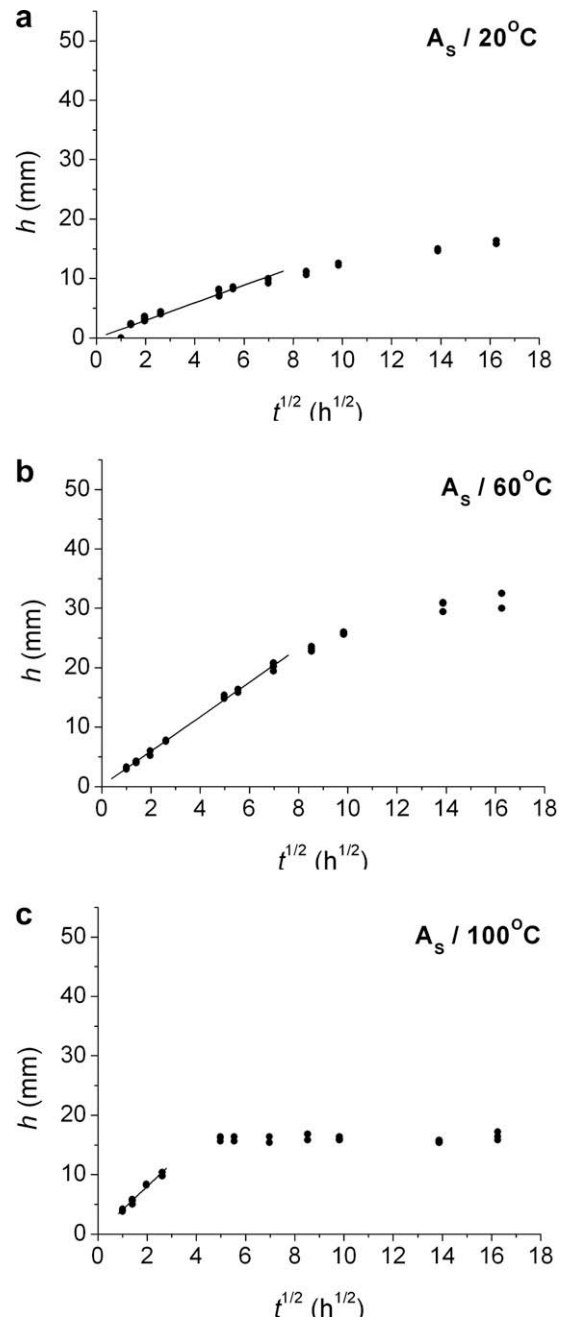


**Fig. 4.** Height of the liquid front ( $h$ ) versus the square root of time ( $t$ ) for a specimen made of concrete with the air-entraining agent *Cementol ETA S* ( $A_S$ ) at: (a) 20 °C; (b) 60 °C and; (c) 100 °C.

The reason for this is that the pores in specimens with an air-entraining agent are larger and therefore less susceptible to capillary absorption. In general it was determined that pores in specimens with an air-entraining agent are filled up to  $\sim 55\%$  and to  $\sim 80\%$  in the other studied cementitious specimens.

Another interesting feature in Fig. 6 is the drop of concentration observed in specimen R at  $\sim 100$  h. Several such drops were observed through the entire study and it is very possible that many others were not detected due to the relatively long time intervals between individual measurements. These drops may be explained as Haines-jumps. Namely, in parts of the specimen which are distant from the immersed surface, the source of liquid is limited. Hence, when liquid accelerates into the above lying pores, the con-

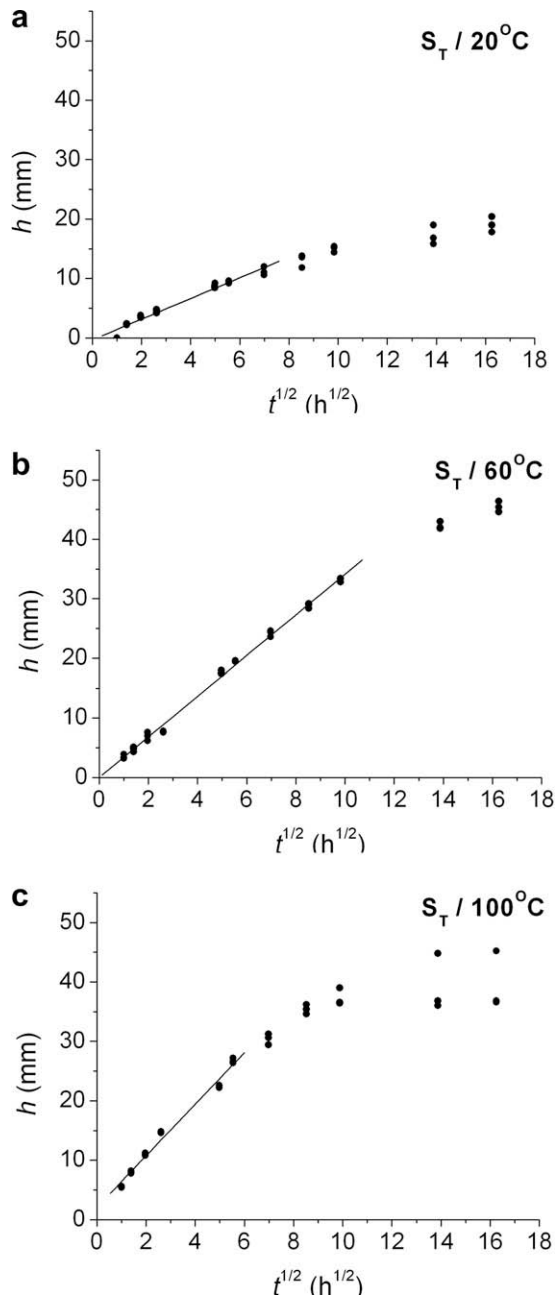


**Fig. 5.** Height of the liquid front ( $h$ ) versus the square root of time ( $t$ ) for a specimen made of concrete with the superplasticizer *Cementol ZETA T* ( $S_T$ ) at: (a) 20 °C; (b) 60 °C and; (c) 100 °C.

**Table 3**

Values of the capillary coefficient ( $k$ ) of ethylene glycol in reference concrete (R), concretes with air-entraining agents ( $A_S$ ,  $A_{S1}$ ) and concretes with superplasticizers ( $S_P$ ,  $S_T$ ) at different temperatures ( $T$ ) as determined by Neutron Radiography. The density ( $\rho$ ) and dynamic viscosity ( $\eta$ ) of ethylene glycol determined by a *Cannon–Fenske* viscometer is given for each temperature.

Mixture	$k$ (mm h <sup>-1/2</sup> )		
	$T = 20\text{ °C}$ $\rho = 1.11\text{ g cm}^{-3}$ $\eta = 23.0\text{ mPa s}$	$T = 60\text{ °C}$ $\rho = 1.09\text{ g cm}^{-3}$ $\eta = 5.2\text{ mPa s}$	$T = 100\text{ °C}$ $\rho = 1.06\text{ g cm}^{-3}$ $\eta = 2.1\text{ mPa s}$
R	1.66	3.47	3.47
$A_S$	1.49	2.90	3.93
$A_{S1}$	1.52	2.82	3.00
$S_P$	1.76	3.81	4.86
$S_T$	1.74	3.41	4.34

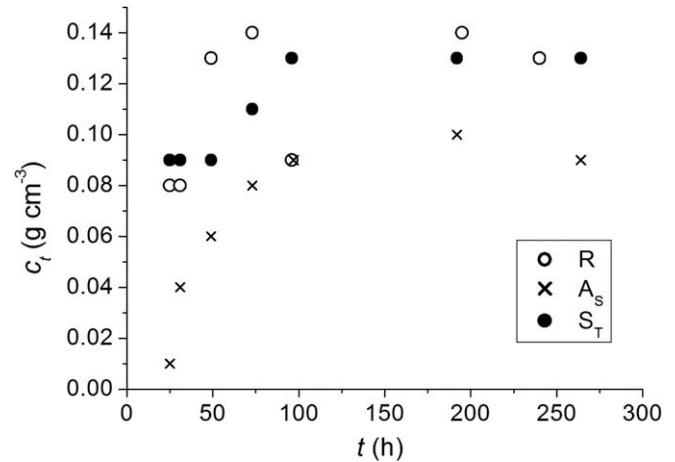


**Fig. 6.** Concentration of ethylene glycol ( $c_l$ ) in reference concrete (R), concrete with the air-entraining agent *Cementol ETA S* ( $A_S$ ) and concrete with the superplasticizer *Cementol ZETA T* ( $S_T$ ) as a function of time ( $t$ ). The concentration was measured at 60 °C in a horizontal profile 15 mm above the bottom edge of the specimen.

**Table 4**

Maximum possible mass concentration ( $c_{l,max}$ ), the highest actually reached concentration ( $c_{l,act}$ ) as determined from Fig. 6, and the portion of pores actually filled with ethylene glycol ( $q_{act}$ ) at 60 °C for reference concrete (R), for concrete with the air-entraining agent *Cementol ETA S* ( $A_S$ ) and for concrete with the superplasticizer *Cementol ZETA T* ( $S_T$ ).

Mixture	$c_{l,max}$ (g cm <sup>-3</sup> )	$c_{l,act}$ (g cm <sup>-3</sup> )	$q_{act}$ (%)
R	0.16	0.14	88
$A_S$	0.22	0.10	45
$S_T$	0.18	0.13	72

centration in the pores below temporarily decreases. These pores are later refilled by the liquid flowing in from lower parts of the specimen.

#### 4. Conclusions

Capillary absorption of ethylene glycol in concrete matrix was monitored and the influence of its porosity and liquid viscosity on absorption kinetics was studied. Different pore distributions in cementitious specimens were achieved by admixtures, namely air-entraining agents and superplasticizers, and compared to a reference mix. The apparent porosity was determined by MIP. Liquid viscosity was altered by the temperature of the system and was measured by a *Cannon–Fenske* viscometer. Values of the capillary coefficient defined by the *Lucas–Washburn* equation used for description of capillary absorption are determined using NR.

The following conclusions are drawn:

- Liquid transport in porous media due to capillary absorption can be divided into three stages: an initial dormant period, a period described by the *Lucas–Washburn* equation and a retarding period, where significant deviation from the *Lucas–Washburn* equation occurs. The latter occurs mostly because the liquid supply is limited in the regions remote from the liquid source.
- The duration of dormant period depends on liquid viscosity and is shorter in the case of low viscosity. At 20 °C the viscosity of ethylene glycol is 22 mPa s and the dormant period is found to be ~1 h.
- For the cementitious materials in combination with ethylene glycol the *Lucas–Washburn* equation is valid for ~25 h.
- Capillary coefficients defined by the *Lucas–Washburn* equation were found to be in the range from 1.5 to 4.9 mm h<sup>-1/2</sup>.

- When the viscosity of ethylene glycol is reduced by a factor of 4, the capillary coefficient increases by a factor of 2.0, whereas it increases by a factor of 2.4 when the viscosity is reduced by a factor of 11.
- In the water-concrete system deviation from the *Lucas–Washburn* equation has previously been assigned to rehydration and swelling of the cement gel. Although this may be one of the reasons, the experiment performed using an organic liquid shows that it is not the main one. The *Lucas–Washburn* equation neglects gravitational forces and even more importantly the fact that the source of liquid in pores distant from the wetted surface is limited.
- A selective pathway of liquid movement is established in porous materials and larger pores remain empty or are filled at later stage of the process. In specimens made with air-entraining agents only ~55% of the pores are filled, whereas this value amounts to ~80% in the reference specimens and specimens with a superplasticizer. The selective pathway is a consequence of the fact that liquid supply inside the specimen is finite and liquid selectively advances through smaller pores where capillary force is large in comparison to counteracting forces. The diameter of pores that are being filled increases with time [8]. Additionally, in larger pores the liquid propagates as a thin layer on the walls of the pore while the central part of the pore remains empty.

### Acknowledgment

Authors acknowledge the kind support of the *Jožef Stefan Institute* in Ljubljana where the experiments using Neutron Radiography and Mercury Intrusion Porosimetry were performed. The paper is written with a warm memory of Prof. Dr. Radomir Ilić, an expert on Neutron Radiography.

### References

- [1] Lucas R. *Kolloid Z* 1918;23(15) (cited in Ref. [8]).
- [2] Washburn EW. *Phys Rev* 1921;17(273) (cited in Ref. [8]).
- [3] Jenkins RG, Rao MB. Effect of elliptical pores on mercury porosimetry results. *Powder Technol* 1984;38:177–80.
- [4] Cook RA, Hover KC. Mercury porosimetry of cement-based materials and associated correction factors. *ACI Mater J* 1993;90(2):152–61.
- [5] Maage M. Frost resistance and pore size distribution in bricks. *Mater Struct* 1984;17(101):345–50.
- [6] Atzeni C, Massidda L, Sanna U. Effect of pore size distribution on strength of hardened cement pastes. In: *Proceedings of 1st international RILEM congress on pore structure and material properties*. Paris: Chapman & Hall; 1987. p. 195–202.
- [7] Reinhardt HW, Gaber K. From pore size distribution to equivalent pore size distribution of cement mortar. *Mater Struct* 1990;23(1):3–15.
- [8] Schoelkopf J, Gane PAC, Ridgway CJ, Matthews GP. Practical observation of deviation from Lucas–Washburn scaling in porous media. *Colloids Surf A: Physicochem Eng Asp* 2002;206(1–3):445–54.
- [9] Butt H-J, Graf K, Kappl M. *Physics and chemistry of interfaces*. Weinheim: Wiley-VCH; 2003.
- [10] Hanžič L, Ilić R. Relationship between liquid sorptivity and capillarity in concrete. *Cem Concr Res* 2003;33(9):1385–8.
- [11] Hearn N, Detwiler RJ, Sframeli C. Water permeability and microstructure of three old concretes. *Cem Concr Res* 1994;24(1):51–61.
- [12] Hall C, Hoff WD, Taylor SC, Wilson MA, Yoon BG, Reinhardt HW, et al. Water anomaly in capillary liquid absorption by cement-based materials. *J Mater Sci Lett* 1995;14(17):1178–81.
- [13] Taylor SC, Hoff WD, Wilson MA, Green KM. Anomalous water transport properties of Portland and blended cement-based materials. *J Mater Sci Lett* 1999;18(23):1925–7.
- [14] Rauch H, Zeilinger A. Hydrogen transport studies using neutron radiography. *Atom Energy Rev* 1977;15(2):249–90.
- [15] Lamarsh JR. *Introduction to nuclear engineering*. Reading: Addison-Wesley; 1977.
- [16] Pel L. *Moisture transport in porous building materials*. PhD thesis. Eindhoven: Technische Universiteit Eindhoven; 1995.
- [17] Kobayashi H, Satoh M. Basic performance of a neutron sensitive photostimulated luminescence device for neutron radiography. *Nucl Instrum Methods Phys Res A* 1999;424(1):1–8.
- [18] Jho C, Carreras M. The effect of viscosity on the drop weight technique for the measurement of dynamic surface-tension. *J Colloid Interface Sci* 1984;99(2):543–8.
- [19] Kaye, Laby. *Tables of physical and chemical constants*. National Physical Laboratory web Ed. <<http://www.kayelaby.npl.co.uk>> (11.09.09).
- [20] EN 197-1. *Cement – Part 1: composition, specifications, and conformity for common cements*; 2000.
- [21] EN 196-1. *Methods of testing cement – Part 1: determination of strength*; 1994.
- [22] Neville AM. *Properties of concrete*. 4th ed. Harlow etc.: Pearson Education; 1995.
- [23] Hanžič L. *Capillarity in concrete*. PhD thesis, Ljubljana, University of Ljubljana; 2005.